

# INNOVATIVE NONDESTRUCTIVE ULTRASONIC TESTING AND ANALYSIS FOR FRP PIPING

Ahmed Arabi Hassen<sup>1</sup>, Uday K. Vaidya<sup>2</sup>, Geoffrey E. Clarkson<sup>3</sup>

<sup>1</sup>*Department of Materials Science and Engineering, Materials Processing & Applications Development (MPAD) Center, University of Alabama at Birmingham, Birmingham, Alabama, USA*

<sup>2</sup>*Department of Mechanical, Aerospace and Biomedical Engineering, University of Tennessee, Knoxville, TN*

<sup>3</sup> UTComp Inc, 260Holiday Inn Drive, Cambridge, ON, CAN N3C4E8

## ABSTRACT

Fiber reinforced plastics (FRP) are being extensively used in chemical vessels, power plants and process piping sectors. Typically these are fabricated via filament winding or hand lay-up and subject to a range of defects such as collection of microvoids, disbonds, fiber misalignment, resin rich/starved areas etc. Access to FRP pipes used in the process and energy industries is oftentimes limited to single side. UTComp utilizes advanced ultrasonic, non-destructive testing technology to acquire data for health monitoring of FRP structures. This data gathered is then evaluated through custom software and analysis. In the present work, FRP pipes ranging from 8" to 24" length and 6" to 8" diameter supplied from number of sources was evaluated by ultrasonic NDE. The FRP pipes were marked in circumferential grids and time domain signals were recorded from 1" diameter ultrasonic transducer of 0.5 MHz resonant frequency transducers in conjunction with an Olympus DL ultrasonic system. The data was reduced by extracting the raw ordered pairs of magnitude and time that constitute the A-scan from a flaw detector. The raw data was further processed to provide prediction of the ratio of actual elastic modulus to theoretical elastic modulus.

## 1. INTRODUCTION

Steel pipelines are known to be the most dominant system for crude oil and gas transportation however; their service life decreases exponentially when they are used in hostile environments such as those with combinations of sulfur, mud, crude, and saltwater. The replacement of the steel pipes by other made from Fiber Reinforced Plastic (FRP) can reduce significant cost. Using FRP piping systems can result in weight savings of an average \$2 to \$4 per pound in construction costs due to their superior lightweight properties and high specific modulus and strength [1]. FRP pipes are corrosion resistant, with low maintenance cost, and long service life [2-4]. The FRP pipe and tank market is expected to have a rapid growth in the next decade. A market study for the North American FRP pipe and tank market showed that the market had a value of \$1.2 billion at 2013 and expected to have a growth of 17% by the year 2019 [5]. In general, FRP pipes are fabricated from corrosion resistant E-glass fibers impregnated with a thermoset resins such as vinyl ester, terephthalic polyester, and epoxy in order to provide high mechanical properties and high temperature operations, up to 260° C (500 °F) [4]. Flame retardant

additives can be added to the FRP piping when they are used to transfer high flammable products such as oil and gas products.

With the FRP pipes market growth and expansion, inspection procedures must be developed for pipes structural health monitoring. However, inspection of composite materials is challenging compared to metals and alloys. Composite materials are anisotropic nature, with poor electrical conductivity, low thermal conductivity, and high acoustic attenuation [4]. Defects can be introduced during different manufacturing stages of composite materials. These defects are commonly occurring because of misapplication of materials, improper installation practice, and poor quality of manufacturing. These defects reflect on the fabricated FRP pipe stiffness and strength. The most common defects found in composite materials are foreign object damage, fiber splitting, fiber fracture, fiber waviness, impact damage, resin micro cracks, pores, and fiber-matrix debonding [6, 7]. In order to avoid any FRP pipe catastrophic failures that could lead to life losses or environmental disaster, these defects should be identified and characterized at early stages. The most common methods for FRP pipe inspection are either visual inspection or pressure testing. The former method often underestimates the risk as the method is subjective and some defects can be missed. In the pressure testing method, the system should be isolated which adds to the inspection cost. FRP pipes can be inspected and evaluated during their fabrication and in service life using Nondestructive Testing (NDT) techniques [4].

Low frequency Ultrasonic Testing (UT) systems and techniques specifically designed for FRP provide rapid and accurate one-sided measurements [8]. UT technique is practical and optimally used for inspecting FRP pipes when representative samples with the laminate type, weight fraction, and fiber orientation are used in the calibration process. Special care should be taken during this process because the FRP pipe surface finish and quality of coupling affects the interpretation of the results. Single-point assessment is not entirely reliable, and not recommended; hence multiple-point inspections are used to map large areas that provide accurate information to characterize the FRP pipes. Multiple-point inspections allow the distribution of defects to be represented using statistical parameters. In addition to identifying defects, UT has also been shown to provide information that relates to characteristics and properties of the FRP [8]. The same readings that may be used to identify defects can be used for the FRP mechanical properties characterization. This paper deals with the use of UT readings as a nondestructive approach to determine modulus properties of FRP pipe sections.

## **2. TYPES OF DEFECTS IN FRP PIPES**

Defects in FRP pipes occur at different stage of the FRP pipe service life. These defects are found commonly due to improper installation practice, misapplication of materials, and poor manufacturing quality. Common defects as porosity, inadequate resin curing, Foreign Object Inclusion (FOI), and dry spot can be found in the fabrication stage. However, defects as impact damage, wear damage, cracks and chalking can be found in installation and service life stages. Full review for typical defects types, cause of the defects and their time of occurrence can be found in [4, 9]. The fabrication and

manufacturing techniques affects the frequency of the defects occurrence in FRP pipes. It can be noticed that in the hand lay-up process results in high levels of porosity, dimensional tolerance limitations, and inconsistent fiber orientations. It was found that centrifugal casted pipes only can be used to process relatively low fiber content FRP pipes, when compared to other fabrication methods, that limits the ultimate pressure obtained at comparable wall thickness. It is worth mention that the filament winding process is the most common method for manufacturing FRP pipes, as it is automated processes that lead to low probabilities of defect existence.

### **3. FRP PIPES INSPECTION METHODS**

There are several inspection technique that can be used for FRP piping health motoring. These techniques are listed in details in [4, 10]. Over estimated factor of safety (i.e. up to 10:1) were used for FRP pipes in early 1970s due to the absence of qualitative and quantitative information at that time. The main purpose for pipe inspection and evaluation is to identify deviations from the design specifications, and perform fast corrective actions to prevent the pipe failure. Common methods of inspection as pressure testing and visual inspection are used to detect high porosity levels and cracks that lead to flow leakage (i.e. drop in the pressure of the transferred fluid or cracks visual to the naked yes). Methods such as Acoustic Emission (AE) can be used in identifying fiber breakage and delamination in composite however, the technique is considered to be an active technique (i.e. the FRP pipe should be under loading). X-ray radiography can be used to detect FOI, fiber waviness, porosity, and crack in FRP, however high safety precautions should be considered and special procedures should be performed (if portable X-ray systems used) to ensure that the induced vibration resulted from the operating pipeline does not affect on the radiographic exposure. Ultrasonic Testing (UT) technique is the most common nondestructive method used in the inspection and characterization of FRP pipes. However, it should be noticed that the inspection of FRP pipes difficult in comparison to other metallic pipes as there are a wide variation of materials and manufacturing procedures used in production of FRP pipes. Low frequency pulse-echo UT systems can be specially designed for FRP pipes inspection that allows rapid and accurate one-sided inspection [8]. There are several defects can be detected using UT method such as plies disbands, cracks porosity and delaminations [6, 11, 12]. In this paper we focus on UT as an inspection method for FRP pipes to evaluate its elastic properties.

## **4. CASE STUDY**

### ***4.1 FRP Pipe Materials and Fabrication***

FRP pipes with 457.2 mm (18“) length and diameters ranging from 101.6mm (4“) to 203.2 mm (8“) were used in this work. The FRP pipes were manufactured from glass fiber / epoxy vinyl ester using filament winding process. These pipes were fabricated from three distinct layers. The first layer is a liner, a smooth layer with special additives that comes with direct contact with the fluid. The main objective of this layer is to provide corrosion and wear resistance for the internal surface of the FRP pipe. The filament layer is the second layer that forms the pipe wall thickness and handles the

stresses resulting from the internal and external pressure. Then a final layer of pure resin coating is added to insure smooth surface finish and full fiber impregnation. Prior knowledge of the fiber weight fraction, ply thickness, and orientation is necessary to obtain reliable UT prediction for the elastic modulus of the FRP pipes. Hence, burn off testing, ply counting and micrographs were performed to obtain this information. Three samples were extracted out the circumferential direction of each pipe and placed in the oven under 500° C for an hour. The samples were weighed before and after the burn off process and the fiber weight fraction ( $W_f$ ) was calculated using the following relation [13],

$$W_{f(Matrix)} = \left( \frac{m_c - m_f}{m_c} \right) \quad (1)$$

$$W_{f(Fiber)} = 1 - W_{f(Matrix)} \quad (2)$$

where  $m_c$  is the total mass of the composite before burn off and  $m_f$  is the mass of the remaining constituent after burn off. After burn off the number of the plies was counted and stereomicroscope (Carl Zeiss Stemi SV11) was used to determine the fiber orientation as shown in Figure 1. Table 1 shows the burn off and plies counting results. The weight fraction values can be converted to volume fraction using the following relation [13],

$$V_f = \frac{W_f \rho_m}{W_f (\rho_m - \rho_f) + \rho_f} \quad (3)$$

where  $\rho_m$  is the matrix density and  $\rho_f$  is the fiber density. The resulted data were used in the theoretical and experimental calculation. The FRP pipes were fabricated from a total of 10 plies The first 6 plies were stacked in  $[-57/+57]_6$  configuration followed by 4 plies of Chopped Strand Mats (CSM) with random orientation. It showed be noticed that the orientation angle values for the unidirectional laminates obtained experimentally has a difference of 2.5° when compered to the reported value by the manufacturer (i.e. -54.5/+54.5). At orientation angles greater than 45°, a minor change in the orientation angle (i.e. 2.5°) does not has a significant effect on the tensile modulus [3].

#### 4.2 Theoretical Evaluation for Elastic Properties of FRP Pipes

Micro-mechanical model can predict the composite stiffness properties from then properties of its original constituents, listed in Table 2. The elastic properties for unidirectional continuous fiber can be calculated using the Rule of Mixture (RoM) [3],

$$E_{11} = E_f (1 - V_m) + E_m V_m \quad (4)$$

$$E_{22} = \frac{E_f E_m}{E_f V_m + E_m (1 - V_m)} \quad (5)$$

where  $E_f$  is the fiber modulus,  $E_m$  is the matrix modulus,  $V_m$  is the matrix volume fraction. However, in this study a modified version of the rule of mixture, see Appendix A, were used to account for the change in the fiber angle. In order to determine the micro-mechanical properties for the CSM with random orientation, the following equation was used [3],

$$E_{CSM} = \frac{3}{8} E_{xx} + \frac{5}{8} E_{yy} \quad (6)$$

where  $E_{xx}$  and  $E_{yy}$  are the longitudinal and transverse tensile modulus for chopped unidirectional fibers respectively obtained by Halpin-Tsai theory [14]. In this case the properties are assumed to be the same in all directions in the plane of the lamina (i.e. isotropic).

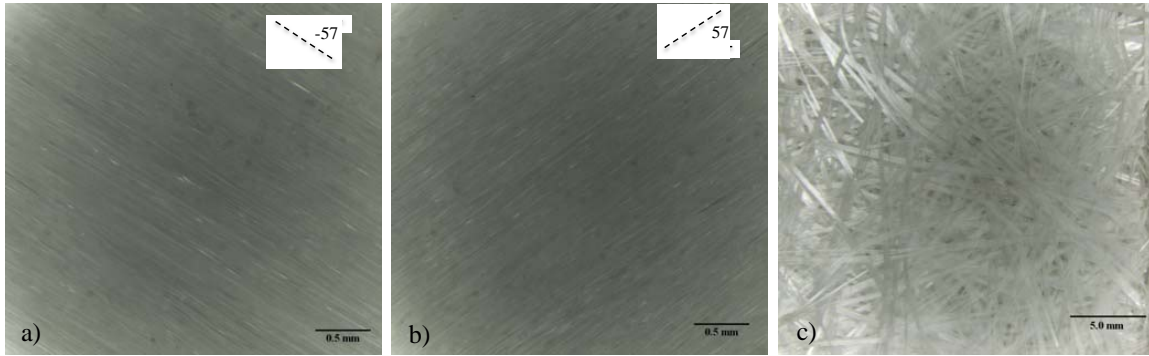


Figure 1: Stereography images for the glass fiber constituent after burn-off; a) Fibers angle of  $-57^\circ$ , b) Fibers angle of  $+57^\circ$ , and c) Fibers with random orientation

Table 1: FRP pipe burn-off and ply counting results

Pipe diameter (mm)	Calculated Fiber volume fraction (%)	Average Fiber Weight fraction (%)	Standard Deviation	Number of Plies
101.6 (4")	34.6	50.8	$\pm 0.8$	3 ply ( $57^\circ$ )
				3 ply ( $57^\circ$ )
152.4 (6")	40.3	56.9	$\pm 0.4$	4 ply (Random)
				3 ply ( $57^\circ$ )
203.2 (8")	39.8	56.4	$\pm 0.7$	3 ply ( $57^\circ$ )
				4 ply (Random)

The elements in the stiffness matrix for an angle ply lamina  $[\bar{Q}_{ij}]$  were determined and then the extensional stiffness matrix and bending stiffness matrix for the laminate was calculated using the Composite Lamination Theory (CLT). For simplicity, the sample assumed to be free from any geometrical curvatures and a perfect interlaminar bond

exists between various laminas. The extensional stiffness matrix [A] and the bending matrix [D] were calculated using the following relations [3],

$$A_{ij} = \sum_{j=1}^N (\bar{Q}_{ij}) (h_j - h_{j-1}) \quad (7)$$

where N is the total number of laminas in the laminate,  $\bar{Q}_{ij}$  elements of the stiffness matrix of the  $j^{\text{th}}$  lamina, and  $h_{j-1}$  is the distance from the mid-plane to the top of the  $j^{\text{th}}$  lamina. The [A] matrix for the FRP pipes can be presented in a matrix form as:-

$$[A] = \begin{bmatrix} A_{11} & A_{12} & A_{13} \\ A_{21} & A_{22} & A_{23} \\ A_{31} & A_{32} & A_{33} \end{bmatrix} \quad (8)$$

Table 3 shows the theoretical elastic modulus values obtained using the CLT [3]. It should be noticed that an increase of 4.5% in the calculated theoretical modulus values for the 4" pipe was observed when compared to the value of 8" FRP; this is attributed to the increase of the fabricated FRP pipe wall thickness.

Table 2: FRP pipes constituent properties

Material	Density (g/cm <sup>3</sup> )	Diameter (μm)	Tensile Modulus (GPa)	Tensile Strength (GPa)	Poisson's Ratio
Glass Fiber (E-glass)	2.54	10 (round)	72.4	3.45	0.2
Epoxy Vinyl Ester	1.3	-	3.2	0.86	0.35

Table 3: Calculated theoretical properties of the FRP pipes<sup>1</sup>

Pipe Diameter (mm)	Total Thickness (mm)	Tensile Modulus (GPa)	Shear Modulus (GPa)
101.6 (4")	5.18	10.103	4.284
152.4 (6")	6.04	11.076	4.909
203.2 (8")	7.09	12.021	5.552

### 4.3 Ultrasonic Testing and Evaluation

In order to obtain a systemic process for measuring and distinguishing the data for each of the given points, a template of a grid system was developed and applied to the provided pipes. The grid system consists of the x-axis (identified by numbers) and y-axis (identified by alphabets) with the origin at the top right. 38.1 mm (1.5") distance between the grid points in both of the circumferential and the longitudinal direction was adapted.

<sup>1</sup> Values provided with contribution from RPS Composites Inc.

Different pipe diameters will result in additional data points of scan in the circumferential direction (i.e. hoop direction) of the pipe. A total of 120, 168 and 228 point were scanned for pipe diameters of 101.6mm (4"), 152.4 (6") and 203.2 mm (8") respectively. Pulse-echo ultrasonic system (Olympus Epoch 4) was used to scan the FRP pipes across the pipe hoop direction. Low frequency flat transducer, 0.5 MHz, with an element diameter of 32 mm (1") coupled with a zero degree vulcanized rubber delay line were used. Readings were taken by holding the transducer in place on the pipe surface and then saving the reading into the memory of the Epoch 4. After all readings were taken, the raw reading data was extracted from the instrument using communications software provided by UTComp. The ultrasonic data was then processed and analyzed remotely using proprietary software owned by UTComp Inc. that calculates the ratio of expected actual modulus to the theoretical modulus from CLT calculations. The ratio is known as the Percentage of Design Strength (PDS). Mathematically, PDS is expressed as,

$$PDS = \frac{\text{Actual Tensile Modulus}}{\text{Theoretical Tensile Modulus}} \quad (9)$$

The UT readings that were taken in the scans of the pipes were combined with pipe ID location, and assembled into a data file that could be processed remotely. The raw data was scaled, normalized and filtered to account for variables in the collection process such as transducer characteristics, pipe geometry and surface conditions and environmental conditions. The original A-scan was transformed to allow quantitative analysis. An example of this transformation is shown in Figure 2. After transformation, the custom program conducted pattern recognition to extract data from the signal reflections from the opposite surface, interfaces or defects within the laminate. The shape of various reflections and the time of their occurrence were analyzed and were used to calculate the shapes and relative magnitudes parameters of the identified signal that were used to determine an attenuation function (L) [8]. This attenuation function describes the distribution and magnitude of the losses from the applied signal over the signal path. The PDS was determined from L and the transit time or FRP thickness for the signal across the full pipe thickness. Table 4 summarizes the results of the UT calculations. The PDS values can be applied to the theoretical modulus values from equation (9) to determine the actual modulus. The theoretical properties in Table 3 assume that the constituent materials are fully mixed with no slip. The UT predictions in Table 4 are based on data obtained directly from the laminates and consider the actual construction, incorporating actual mixing and bonding of the constituent materials.

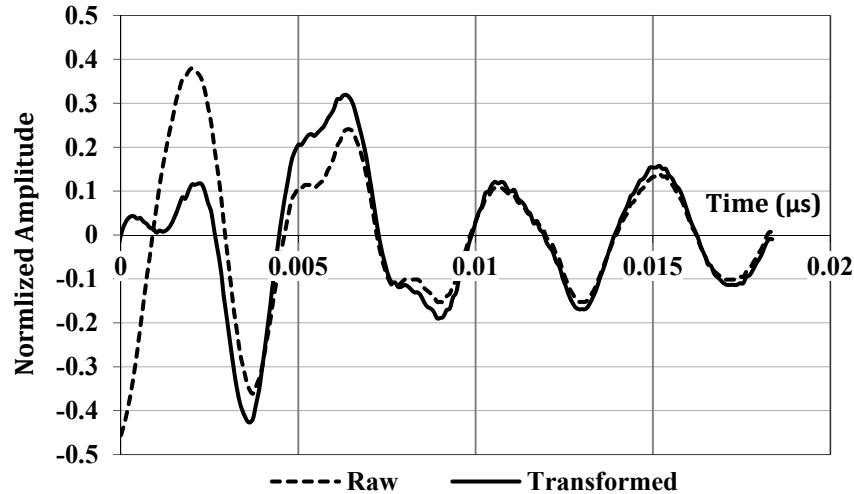


Figure 2: Raw and transformed reading

Table 4: Developed ultrasonic method results summary

Pipe Diameter	PDS Calculated Using Signal Transit Time			PDS Calculated Using FRP Thickness		
	Average (%)	Standard Deviation (%)	Predicted Hoop Modulus (GPa)	Average (%)	Standard Deviation (%)	Predicted Hoop Modulus (GPa)
101.6 (4")	125	±13	12.63	125	±14	12.63
152.4 (6")	102	±15	11.27	102	±17	11.29
203.2 (8")	124	±15	14.91	113	±16	13.64

#### 4.4 Hoop Modulus Testing

A split ring test was conducted to determine the hoop modulus using (MTS-222 kN) hydraulic testing frame following test standard ASTM D2290, as shown in Figure 2. In this test the FRP pipe was sliced to sections with a width of approximately 38 mm (1.5") and then mounted on a universal tensile machine using a special testing fixture. The rings were subjected to loading and unloading cycle at a constant loading rate of 3 mm/min. Strain gages were mounted on the FRP pipes outer diameter along the hoop direction, see Figure 2, to determine the corresponding strain. The maximum load kept always below the yield strength of the composite and the modulus was calculated from the linear regression analysis of the stress strain curve. An average of three rings per each pipe diameter were reported. All pipe rings were tested under elastic deformation and no permanent deflection was applied to the samples. Table 5 show the split ring testing values for two different FRP pipes with diameter of 6" and 8". The average values for three different rings for each FRP pipe diameter were reported. It can be noticed from Table 5 that the UT method has the ability to predict the Hoop modulus accurately. Only a difference of 9.4% and 2.1% in the predicted modulus value was observed when compared to the experimental value obtained by the split ring testing for FRP pipes with



6” and 8” diameter respectively. These differences are less than the range from the destructive tests.

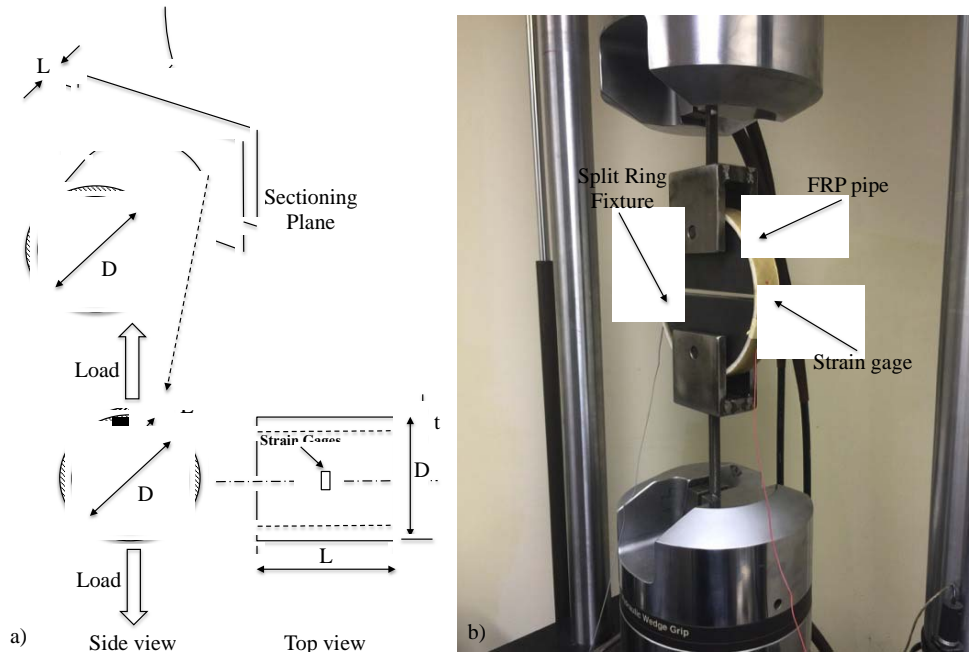


Figure 3: FRP split ring testing, a) Schematic for split ring testing showing loading direction and the strain gages attached, and b) Actual split ring testing setup

Table 5: Comparison of Hoop tensile modulus obtained by spit ring testing and Hoop tensile modulus obtained by non-destructive testing

Pipe diameter (mm)	Spit Ring Hoop Tensile Modulus (GPa)	Predicted Hoop Tensile Modulus (GPa)
152.4 (6")	10.3 ± 1.3	11.27 ± 1.7
203.2 (8")	14.6 ± 0.97	14.91 ± 2.2

## 5. CONCLUSION

FRP pipes are on the rise due to their superior corrosion resistance, lightweight and high strength-to-weight ratio, which makes them attractive to be used in many industrial product applications. Prior knowledge of FRP piping defects, methods of inspection and FRP pipe material characterization prevents any unexpected failures. These defects affect the structural integrity of FRP pipes and their mechanical properties. Different methods and strategies for FRP pipe inspection can be used however UT inspection methods proved advantages over other method in terms of reliability, portability (in field use) and easiness. The ultrasonic method used in this paper is known as the UTComp<sup>®</sup> System and provides non-destructive assessment of the structural capacity of FRP piping systems. The method uses easily available instruments along with a short training cycle and highly automated data processing, thereby reducing inspector skill requirements. This paper shows that the method determines the actual structural capacity of FRP piping.

## 6. REFERENCES

1. Curran, S., *Fiberglass Pipe Past, Present and Future*. 2013, Fiberglass Tank & Pipe Institute: Houston, TX.
2. Ning, H., S. Pillay, and U.K. Vaidya, Design and development of thermoplastic composite roof door for mass transit bus. *Materials & Design*, April, 2009. **30**(4): p. 983-991.
3. Mallick, P.K., *Fiber reinforced composites: Materials, Manufacturing, and Design*. 2008, New York, USA: Taylor and Francis Group.
4. Ahmed Arabi Hassen, U.K. Vaidya, and Frank Britt, Structural Integrity of Fiber Reinforced Plastic Piping. *Material Evaluation*, , 2015. **73**(7): p. 919-929.
5. Aylward, P., Pipe and Tank Market Poised for Growth, in *composites manufacturing*. September 1, 2014, American Composites Manufacturers Association (ACMA): USA.
6. Ahmed Arabi Hassen, et al. Tracing Defects in Glass Fiber/Polypropylene Composites Using Ultrasonic C-Scan and X-Ray Computed Tomography Methods. in *ASNT Annual Conference*. October, 2014. Charleston, SC, USA: ASNT.
7. T. Khan, et al., Novel Damage Diagnosis Algorithms for Aerospace Nondestructive Testing Data Using Ultrasonic Testing Technique, in *ASNT 23rd Research Symposium*, ASNT, Editor. March, 2014: Minneapolis, MN, USA. p. 67-71.
8. Clarkson, G.E. Baseline Values for Non-Destructive Structural Evaluation of Glass Reinforced Composites. in *The Composites and Advanced Materials Expo., CAMX*. 2014. Orlando, FL, USA: CAMX.
9. Norwegian Oil and Gas Association, 055 – Norwegian Oil and Gas Recommended Guidelines for NDT Of GRP Pipe Systems and Tanks. 1997: Norway.
10. Summerscales, J., *Non-Destructive Testing of Fibre-Reinforced Plastics Composites*. 1987, UK: Elsevier applied science
11. Theodoros, H., B. Efstratios, and G.T. Nicolaos, Application of Ultrasonic C-Scan Techniques for Tracing Defects in Laminated Composite Materials. *Journal of Mechanical Engineering*, 2011. **57**(3): p. 192-203.
12. Li, S., et al. Defect Mapping Based on Signal Correlation for Ultrasonic NDE. in *ASNT 2013 Fall Conference*. 2013. Las Vegas, NV, USA.
13. Shao-Yun Fu, B. Lauke, and Y.W. Mai, *Science and engineering of short fibre reinforced polymers composites*. 2009, Cambridge, UK Woodhead Publishing.
14. Halpin, J.C. and J. Kardos, The Halpin-Tsai equations: a review. *Polymer engineering and science*, 1976. **16**(5): p. 344-352.

## 7. ACKNOWLEDGEMENTS

The authors acknowledge contributions of pipe samples and construction details supplied by RPS Composites.